Cholecystokinin release triggered by NMDA receptors produces LTP and sound–sound associative memory

Xi Chen[a,b,1], Xiao Li[a,b,1], Yin Ting Wong[a,1], Xuejiao Zheng[a,b,c], Haitao Wang[d], Yujie Peng[a,b], Hemin Feng[a], Jingyu Feng[a], Joewel T. Baibado[a], Robert Jesky[a], Zhedi Wang[a,b], Hui Xie[a], Wenjian Sun[a], Zicong Zhang[a], Xu Zhang[a], Ling He[a,b,e], Nan Zhang[a,b], Zhijian Zhang[c], Peng Tang[a,b], Junfeng Su[a], Ling-Li Hu[d], Qing Liu[c], Xiaobin He[c], Ailian Tan[a,b], Xia Sun[f], Min Li[a,b,c], Kelvin Wong[a], Xiaoyu Wang[a,b], Hon-Yeung Cheung[a], Daisy Kwok-Yan Shum[g,h], Ken K. L. Yung[i], Ying-Shing Chan[g,h], Micky Tortorella[d], Yiping Guo[d], Fuqiang Xu[c], and Jufang He[a,b,2]

[a]Department of Biomedical Sciences, City University of Hong Kong, Kowloon Tong, Hong Kong; [b]City University of Hong Kong Shenzhen Research Institute, 518057 Shenzhen, China; [c]Center for Brain Science, State Key Laboratory of Magnetic Resonance and Atomic Molecular Physics, Key Laboratory of Magnetic Resonance in Biological Systems, Wuhan Institute of Physics and Mathematics, Chinese Academy of Sciences, 430071 Wuhan, China; [d]Key Laboratory of Regenerative Biology, Guangzhou Institute of Biomedicine and Health, Chinese Academy of Sciences, 510530 Guangzhou, China; [e]School of Life Sciences, Harbin Institute of Technology, 150006 Harbin, China; [f]School of Medicine, Hangzhou Normal University, 310018 Hangzhou, China; [g]School of Biomedical Sciences, Li Ka Shing Faculty of Medicine, The University of Hong Kong, Hong Kong; [h]State Key Laboratory of Brain and Cognitive Science, The University of Hong Kong, Hong Kong; and [i]Department of Biology, Hong Kong Baptist University, Kowloon Tong, Hong Kong

Edited by Michael P. Stryker, University of California San Francisco Medical Center, San Francisco, CA, and approved February 4, 2019 (received for review September 29, 2018)

Memory is stored in neural networks via changes in synaptic strength mediated in part by NMDA receptor (NMDAR)-dependent long-term potentiation (LTP). Here we show that a cholecystokinin (CCK)-B receptor (CCKBR) antagonist blocks high-frequency stimulation-induced neocortical LTP, whereas local infusion of CCK induces LTP. $CCK^{-/-}$ mice lacked neocortical LTP and showed deficits in a cue–cue associative learning paradigm; and administration of CCK rescued associative learning deficits. High-frequency stimulation-induced neocortical LTP was completely blocked by either the NMDAR antagonist or the CCKBR antagonist, while application of either NMDA or CCK induced LTP after low-frequency stimulation. In the presence of CCK, LTP was still induced even after blockade of NMDARs. Local application of NMDA induced the release of CCK in the neocortex. These findings suggest that NMDARs control the release of CCK, which enables neocortical LTP and the formation of cue–cue associative memory.

cholecystokinin | NMDA receptor | long-term potentiation | memory | entorhinal cortex

Memory is stored in neural networks through changes in synaptic strength (1). Long-term potentiation (LTP) and long-term depression (LTD) are two forms of synaptic plasticity that are believed to represent a neural basis of memory in different brain regions (2–5). The major form of LTP in the hippocampus and neocortex is induced through theta burst stimulation or high-frequency stimulation (HFS) (2, 3). Previous studies have shown that NMDA receptors (NMDARs) play a crucial role in HFS-induced LTP in the hippocampus (6–9) and neocortex (2, 10), and in the formation and consolidation of associative memory (11, 12).

Serving as the gateway from the hippocampus to the neocortex, the entorhinal cortex forms strong reciprocal connections with the neocortex (13, 14) and shows extensive cholecystokinin (CCK) labeling (15–17) with projections to neocortical areas, including the auditory cortex (13, 14, 18). CCK is the most abundant cortical neuropeptide (19), and mice lacking the CCK gene exhibit poor performance in a passive avoidance task and display impaired spatial memory (20). Although many studies have focused on GABAergic CCK neurons (21–24), many glutamatergic neurons in the neocortex express CCK (25, 26). We previously found that local infusion of CCK into the auditory cortex of anesthetized rats induces plastic changes that enable auditory cortical neurons to start responding to a light stimulus after its pairing with an auditory stimulus (18). Activation of the entorhinal cortex potentiates neuronal responses in the auditory cortex, and this effect is suppressed by infusion of a CCK-B receptor (CCKBR) antagonist (18), suggesting that the entorhinal cortex enables neocortical plasticity via CCK-containing neurons projecting to the neocortex.

If CCK enables cortical neuroplasticity and associative memory formation, then we would expect CCK-induced neuroplasticity to affect LTP. The release of neuropeptides occurs slowly in response to repetitive firing (27, 28). Therefore, we hypothesize that HFS activates both postsynaptic neurons and presynaptic terminals, including those containing CCK. The activation, in turn, leads to CCK release and LTP induction in the neocortex. Indeed, our work has shown that CCK enables cortical neuroplasticity and associative memory formation, which correlates with the emerging insight that CCK plays a role in triggering LTP (18). NMDARs participate in the formation of HFS-induced LTP (29, 30). Thus, we further hypothesized that the release of CCK is controlled by NMDARs.

In the present study, we used optogenetic stimulation, in vivo extracellular recordings, in vitro extracellular and intracellular recording, and behavioral testing to examine: (*i*) the role of CCK released from the entorhinal cortex on neocortical LTP induction

Significance

Neuropeptides represent the most diverse family of neurotransmitters with a wide distribution in the rodent brain. Cholecystokinin (CCK) is an octapeptide present in very high concentrations in the cortex, where it is expressed in several circuits. It has emerged as a useful marker, for example as an interneuron subpopulation, but its function is still unclear. Here we show that CCK, via its CCKB receptor, is essential for high-frequency stimulation-induced long-term potentiation, and that release of CCK is controlled by NMDA receptors. Thus, CCK may play an important role in memory formation.

Author contributions: X.C., X.L., F.X., and J.H. designed research; X.C., X.L., Y.T.W., X. Zheng, H.W., Y.P., H.F., J.F., J.T.B., R.J., Z.W., H.X., W.S., Zicong Zhang, X. Zhang, L.H., N.Z., Zhijian Zhang, P.T., J.S., L.-L.H., Q.L., X.H., A.T., X.S., M.L., K.W., X.W., H.-Y.C., D.K.-Y.S., K.K.L.Y., Y.-S.C., M.T., Y.G., and F.X. performed research; X.C., X.L., Y.T.W., X. Zheng, H.W., Y.P., H.F., J.F., J.T.B., R.J., Z.W., H.X., W.S., Zicong Zhang, X. Zhang, L.H., N.Z., Zhijian Zhang, P.T., J.S., L.-L.H., Q.L., X.H., A.T., X.S., M.L., K.W., and X.W. analyzed data; and X.C., X.L., and J.H. wrote the paper.

The authors declare no conflict of interest.

This article is a PNAS Direct Submission.

[1]X.C., X.L., and Y.T.W. contributed equally to this work.

[2]To whom correspondence should be addressed. Email: jufanghe@cityu.edu.hk.

This article contains supporting information online at www.pnas.org/lookup/suppl/doi:10.1073/pnas.1816833116/-/DCSupplemental.

Published online March 8, 2019.

and cue–cue associative memory formation, and (*ii*) the relationship between CCK release and NMDARs.

Results

Role of CCK in in Vivo Neocortical LTP Induction. An in vivo LTP model was first established in the auditory cortex of the rat to investigate the relationship between the CCK-enabled neuroplasticity and neocortical LTP (Fig. 1 *A–D*). We inserted stimulating and recording electrodes into the auditory cortex of the anesthetized rat. Field excitatory postsynaptic potentials (fEPSPs) were recorded from the recording electrode while electrical-pulse stimulation (ES) of different currents was delivered to the stimulating electrode. We adopted 50% of the current that evoked the maximal fEPSP as the testing current and 75% as the HFS current. We confirmed that HFS readily induced LTP (Fig. 1 *C* and *D*) [one-way ANOVA with repeated measures (RM), $F(1, 69) = 125.3$, $P < 0.001$, $n = 14$ from 5 rats].

Previously, we proposed that CCK acts as a chemical switch that enables neuroplasticity (18). Here we hypothesized that HFS induces CCK release, which leads to cortical LTP induction. To test this hypothesis, we used microdialysis and ELISA to measure the concentration of CCK in the cerebrospinal fluid (CSF) before and after HFS in the auditory cortex (Fig. 1*E*). CCK concentration increased from undetectable (<1 pg/mL) before to 5.37 ± 1.00 pg/mL during the first 30 min after HFS in the auditory cortex (Fig. 1*F* and *SI Appendix*, Fig. S1) [one-way RM ANOVA with a Greenhouse–Geisser correction, $F(1.1, 6.6) = 20.2$, $P = 0.003$, $n = 7$ from 5 rats; pairwise comparison, before vs. first 30 min after the HFS, $P = 0.021$] , and recovered to 0.55 ± 0.24 pg/mL in the second 30-min interval after HFS.

To test our hypothesis that CCK is the chemical switch for LTP induction, we infused a CCKBR antagonist, L365,260, and vehicle control, artificial CSF (ACSF), into the auditory cortex before the HFS (Fig. 1*G*). We found that infusion of L365,260 blocked LTP induction, whereas infusion of the vehicle did not affect LTP induction [two-way RM ANOVA, significant interaction, $F(3, 288) = 22.1$, $P < 0.001$; pairwise comparison, L365,260 vs. vehicle 1 h after the HFS, 93.2 ± 2.7% vs. 131.8 ± 2.7%, $P < 0.001$; for L365,260, $n = 10$ hemispheres from 8 rats, for vehicle, $n = 12$ from 11 rats] (Fig. 1 *H* and *I* and *SI Appendix*, Fig. S2). In L365,260-infused rats, there was no significant change in the slope of fEPSPs after the HFS (pairwise comparison, $P = 0.241$). In contrast, in vehicle-infused rats, the fEPSP slope increased by 32.7 ± 2.8% after the HFS (pairwise comparison, $P < 0.001$).

The experiments in Fig. 1 *E–I* indicate that HFS induces CCK release. To further test the role of CCK and its relationship with HFS in cortical LTP induction, we replaced HFS with an infusion of CCK in the area between the stimulating and recording electrodes (Fig. 1*J*) and low-frequency stimulation (LFS; at 0.1 Hz), which presumably evoked pre- and postsynaptic activation. CCK infusion without HFS induced LTP in the auditory cortex of rats [two-way RM ANOVA showed significant interaction, $F(1, 98) = 64.4$, $P < 0.001$; pairwise comparison, before vs. after CCK infusion, $P < 0.001$, $n = 10$ from 10 hemispheres of 6 rats] (Fig. 1 *K* and *L*), whereas no LTP was induced by vehicle infusion (pairwise comparison, before vs. after ACSF infusion, $P = 0.13$, $n = 10$ from 2 rats).

LTP and Memory Deficits in CCK$^{-/-}$ and CCK-Suppressed Mice. Genetic modification has better specificity than antagonists to CCK receptors. In the following experiments, we adopted CCK-Cre [Cck$^{tm1.1(Cre)Zjh/J}$] and CCK-CreER [CCK$^{-/-}$, Cck$^{tm2.1(Cre/ERT2)Zjh/J}$] mice (see *SI Appendix*, Fig. S3*A* for detailed information of both mice). With the CCK-Cre mice, we are able to transfect the CCK^{+} neurons in our targeted area, the entorhinal cortex, with adeno-associated virus (AAV) in our later experiments. No CCK mRNA variant 1 could be detected in CCK$^{-/-}$ mice, while CCK-Cre mice showed a decreased level of CCK mRNA variant 1 in their entorhinal cortex (35.8 ± 6.5% relative to C57 mice) (*SI Appendix*, Fig. S3*B*).

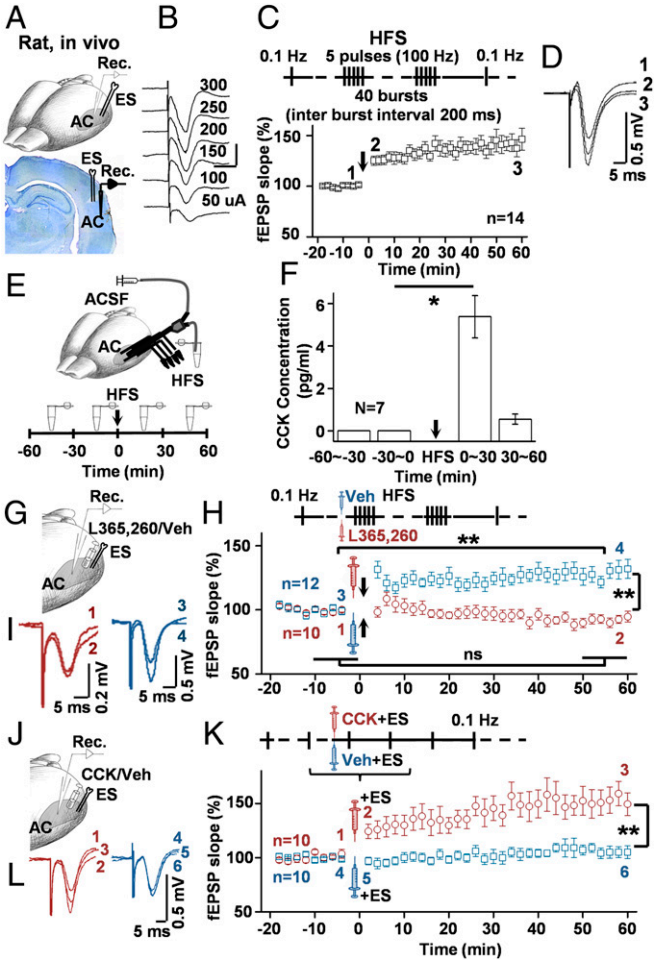

Fig. 1. Role of CCK in neocortical LTP induction on the rats. (*A*) Position of recording and stimulating electrodes in the auditory cortex of rats. (*B*) Representative relationship between input currents and evoked fEPSPs. (*C*) Normalized slopes of fEPSPs before and after HFS. HFS paradigm above the curve. (*D*) Representative single fEPSP traces before (1, just before HFS) and after HFS (2, just after HFS; 3, at the end of the recording, corresponding to the numbers indicated in *C*). (*E*) Diagram of stimulation electrode placements and microdialysis with a schedule showing time points of ACSF collection and HFS application. (*F*) A bar chart showing concentrations of CCK before and after HFS in the auditory cortex based on ELISA. At the baseline level, from –60 min to 0 min, the concentration of CCK was lower than the detection limit (1 pg/mL), set as 0. After HFS, the concentration of CCK increased to 5.37 ± 1.15 pg/mL (one-way RM ANOVA, $*P = 0.021$), but dropped quickly in the following half hour. (*G*) Positions of recording and stimulating electrodes and pipette in the auditory cortex of rats. (*H*) Normalized slopes of fEPSPs before and after HFS with L365,260 (red circle) or vehicle (blue square) injection (two-way RM ANOVA, $**P < 0.001$). HFS protocol above the curve. Bars at the bottom indicate the periods over which the data are being pooled for the before and after measurements. (*I*) Representative single fEPSP traces before and after injection of L365,260 (1-2, at the end of each recording period) or vehicle (3-4, at the end of each recording period) and HFS. (*J*) Positions of recording and stimulating electrodes and pipette in the auditory cortex of rats. (*K*) Normalized slopes of fEPSPs before and after CCK (red circle) or vehicle (blue square) injection (two-way RM ANOVA, $**P < 0.001$). The experimental protocol above the curve. (*L*) Representative single fEPSP traces before and after injection of CCK (1–3) or vehicle (4–6). Data are expressed as mean ± SEM. AC, auditory cortex; Rec., recording electrode; Veh, vehicle.

If CCK acts as a chemical switch that enables neocortical neuroplasticity, then we would expect deficits in neocortical LTP in CCK$^{-/-}$ mice. Indeed, no LTP was induced by HFS in the

auditory cortex of CCK$^{-/-}$ mice [two-way RM ANOVA, significant interaction $F(1, 178) = 112.5$, $P < 0.001$; pairwise comparison, before vs. after HFS, $P = 0.52$, $n = 20$ from 20 mice] (Fig. 2 *A–C*), whereas wild-type C57 mice showed significant HFS-induced LTP (pairwise comparison, before vs. after HFS, $P < 0.001$, $n = 16$ from 16 mice). Importantly, CCK$^{-/-}$ mice neurons in the auditory cortex responded to auditory stimuli and produced event-related potentials similar to the wild-type mice (*SI Appendix*, Fig. S4), indicating that the auditory pathway was functionally intact in CCK$^{-/-}$ mice.

Infusion of CCK in the neocortex of CCK$^{-/-}$ mice rescued LTP, indicating that CCK receptors in CCK$^{-/-}$ mice are functional (*SI Appendix*, Fig. S5 *A–C*). To determine whether the lack of LTP in CCK$^{-/-}$ mice is associated with impaired learning and memory, we tested for the formation of associative memory between two auditory stimuli: that is, cue–cue association. We assumed that mice would be able to associate the cues after presenting them (tone f1 and tone f2; 3 s each) in sequence with an interval of 500 ms in between and a 30-s intertrial interval for a total of 300 trials for 3 d (100 trials comprised of four 25-trial sessions per day). The rationale to put the interval between tones was to avoid the posttone inhibition from tone f1 on neuronal responses to tone f2. We have considered the possibility that cortical inhibition is compromised in CCK$^{-/-}$ mice due to disruption of the CCK signaling pathway, and hence that the response to tone f2 is masked by the preceding tone f1. We recorded responses to tone f1 and f2 presented in sequence in the auditory cortex of CCK$^{-/-}$ and wild-type mice. It was found that neurons in the auditory cortex of CCK$^{-/-}$ mice responded in a similar way as in wild-type mice (*SI Appendix*, Fig. S6). Therefore, responses to two tones presented in sequence are not altered in CCK$^{-/-}$ mice. We then conditioned the tone f2 with the footshock on day 4. We expected that mice would show a fear response not only to tone f2 but also to tone f1, as mice would associate tone f1 with tone f2. In the first experiment, we compared the formation of associative memory following the paradigm noted above in CCK$^{-/-}$ and C57 mice (Fig. 2*D*). Both mice showed low freezing percentages for all three tones before the fear conditioning. The C57 mice showed a significantly higher freezing percentage to tone f1 (1 kHz) that was paired with f2 (4 kHz) than to tone f3 (16 kHz), which was not previously paired with f2 [55.0 ± 7.6% vs. 16.3 ± 4.9%, two-way RM ANOVA, significant interaction $F(2, 22) = 24.7$, $P < 0.001$; pairwise comparison, f1 vs. f3 postconditioning, $P = 0.004$, $n = 12$] (Fig. 2*E* and Movie S1), indicating that an associative memory was formed between the f1 and f2 tones after 300 paired trials in C57 mice. While the difference between the freezing percentages to f1 and f3 was not statistically significant on CCK$^{-/-}$ mice [21.0 ± 5.0% vs. 17.0 ± 4.0%, two-way RM ANOVA with a Greenhouse–Geisser correction, significant interaction $F(1.2, 11.1) = 43.5$, $P < 0.001$; pairwise comparison, f1 vs. f3 postconditioning, $P = 1$, $n = 10$] (Fig. 2*F* and Movie S2), the conditioning trials required for the CCK$^{-/-}$ to achieve the same freezing percentage as the C57 mice were three times more (nine vs. three).

In the second experiment, we compared the influence of the infused CCKBR antagonist in the auditory cortex during tone f1 and f2 pairing on the formation of associative memory in C57 mice, following the same associative memory paradigm as mentioned above (Fig. 2*G*). Mice that received a bilateral infusion of L365,260 in the auditory cortex showed no freezing (Movie S3), while those with vehicle infusion (ACSF in DMSO) showed a significant amount of freezing time when f1 was presented [56.7 ± 5.1% vs. 0 ± 5.1%, three-way RM ANOVA, significant interaction $F(1, 10) = 12.8$, $P = 0.005$; pairwise comparison, post-f1 vehicle vs. L365,260, $P < 0.001$; $n = 6$ for ACSF group; $n = 6$ for L365,260 group] (Fig. 2*H* and Movie S4). A third tone was adopted as another control for f1, (*SI Appendix*, Fig. S7). No infusion was performed during pre- and posttreatment testing.

In the third experiment, we infused a CCK agonist, CCK-4, through an implanted cannula in the venous sinus on the scalp of CCK$^{-/-}$ mice (*SI Appendix*, Fig. S5*D*). Infusion of CCK-4 enabled the formation of associative memory in CCK$^{-/-}$ mice, rescuing the associative memory deficit in CCK$^{-/-}$ mice. However, neither infusion of saline or NMDA (1.5 mM in saline) improved the freezing time after the presentation of f1 (*SI Appendix*, Fig. S5*E*).

Pairing Neuronal Firing with Simultaneous Puff-Applications of CCK and Glutamate in Cultured Cortical Neurons Potentiates Postsynaptic Currents. To determine whether LTP could be independently

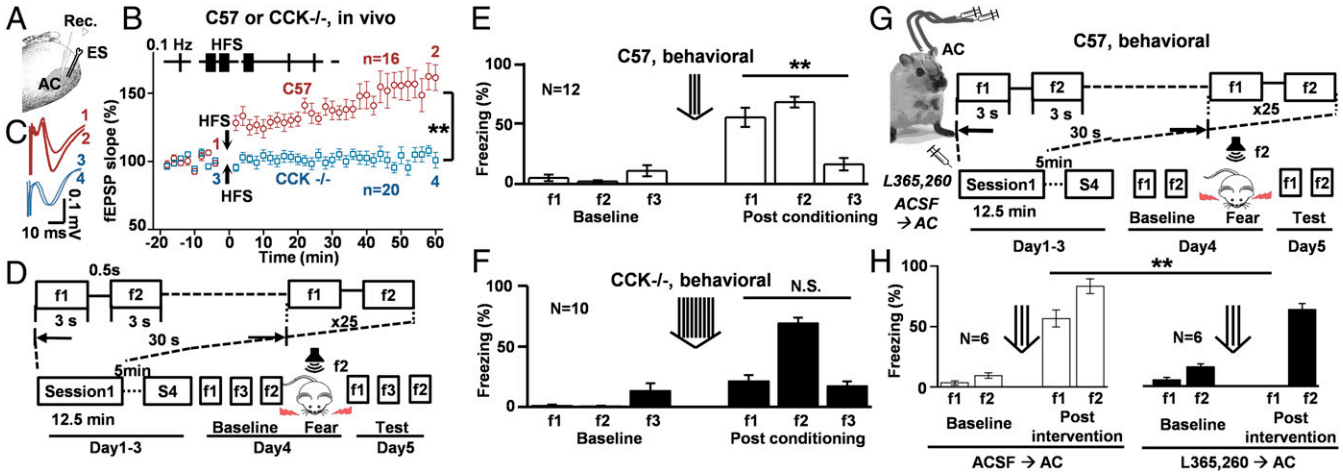

Fig. 2. Neocortical LTP and learning an association between two tones were eliminated in CCK$^{-/-}$ mice. (*A*) Positions of recording and stimulating electrodes in the mouse auditory cortex. (*B*) Normalized slopes of fEPSPs before and after HFS in C57 mice (red circle) or CCK$^{-/-}$ mice (blue square) (two-way RM ANOVA, $^{**}P < 0.001$). HFS protocol above the curve. (*C*) Representative single fEPSP traces before and after HFS in C57 mice (1, 2) and CCK$^{-/-}$ mice (3, 4). (*D*) Diagram of a training protocol for mice to associate the tones of f1 and f2. (*E* and *F*) Bar charts show freezing percentages of the C57 mice (open, *E*) and CCK$^{-/-}$ mice (shaded, *F*) to tones of f1, f2, and f3, before and after the conditioning (two-way RM ANOVA, $^{**}P < 0.001$). (*G*) A training protocol for C57 mice to associate the tones of f1 and f2. The sketch shows implanted drug infusion cannulas in both sides of the auditory cortex. (*H*) Bar charts show freezing percentages of the C57 mice with ACSF infusion (open) and with L365,260 infusion (shaded) to tones of f1 and f2, before and after the conditioning (one-way RM ANOVA, $^{**}P < 0.001$). Data are expressed as mean ± SEM. N.S., not significant.

produced postsynaptically, we adopted glutamate puffing to directly activate glutamate receptors and CCK puffing to activate CCKBRs at the postsynaptic membrane of cultured cortical neurons. Cultured cortical neurons showed no direct change in membrane potential to CCK puffing in a time window of tens of seconds or to repeated applications of CCK in a short time window within a second (see Fig. 3*A* for the preparation and *SI Appendix*, Fig. S8 *A–H*). However, the neuron responded to glutamate puffing at the soma or dendrites (Fig. 3*B*, baseline) without action potential due to the small amount of each puffing. Based on our previous in vivo intracellular recordings, three conditions, including (*i*) the presence of CCK, (*ii*) presynaptic, and (*iii*) postsynaptic coactivities must be fulfilled to produce synaptic plasticity (18). Given that memories can be rapidly formed in the mammalian brain, we hypothesized that synaptic plasticity would happen after a few pairing trials. To test this hypothesis, we paired depolarizing current injections of the recorded neuron with simultaneous puff-applications of glutamate and CCK for three trials (Fig. 3*B*). The glutamate-activated current changed from 129.9 pA before the pairing to 222.4 pA at 5 min, 223.8 pA at 10 min, 242.8 pA at 30 min, and 230.1 pA at 60 min after the pairing (Fig. 3*B*). Population data showed a significant increase in glutamate-activated current after the pairing [two-way RM ANOVA, significant interaction $F(1, 83) = 117.2$, $P < 0.001$; increased by 47.0 ± 2.7%, pairwise comparison, before vs. after paring, $P < 0.001$, $n = 11$ neurons] (Fig. 3*C*; see *SI Appendix*, Fig. S9 for two examples), while simple glutamate puffing without pairing induced no potentiation in the current (pairwise comparison, before vs. after puffing, $P = 0.63$, $n = 6$) (Fig. 3*C*). In another control experiment, pairing the glutamate puffing with the depolarization of the recorded neuron for three trials without CCK application did not induce a potentiation in the glutamate-activated current (*SI Appendix*, Fig. S8 *I* and *J*). These data clearly demonstrate the postsynaptic nature of the CCK-induced potentiation.

HFS Laser Activation of Entorhinal CCK Projections Induces LTP in Patched Neurons in Neocortical Slices. Up to this point, we have established the link between CCK and neocortical LTP. In the next experiment, we investigated the relationship between

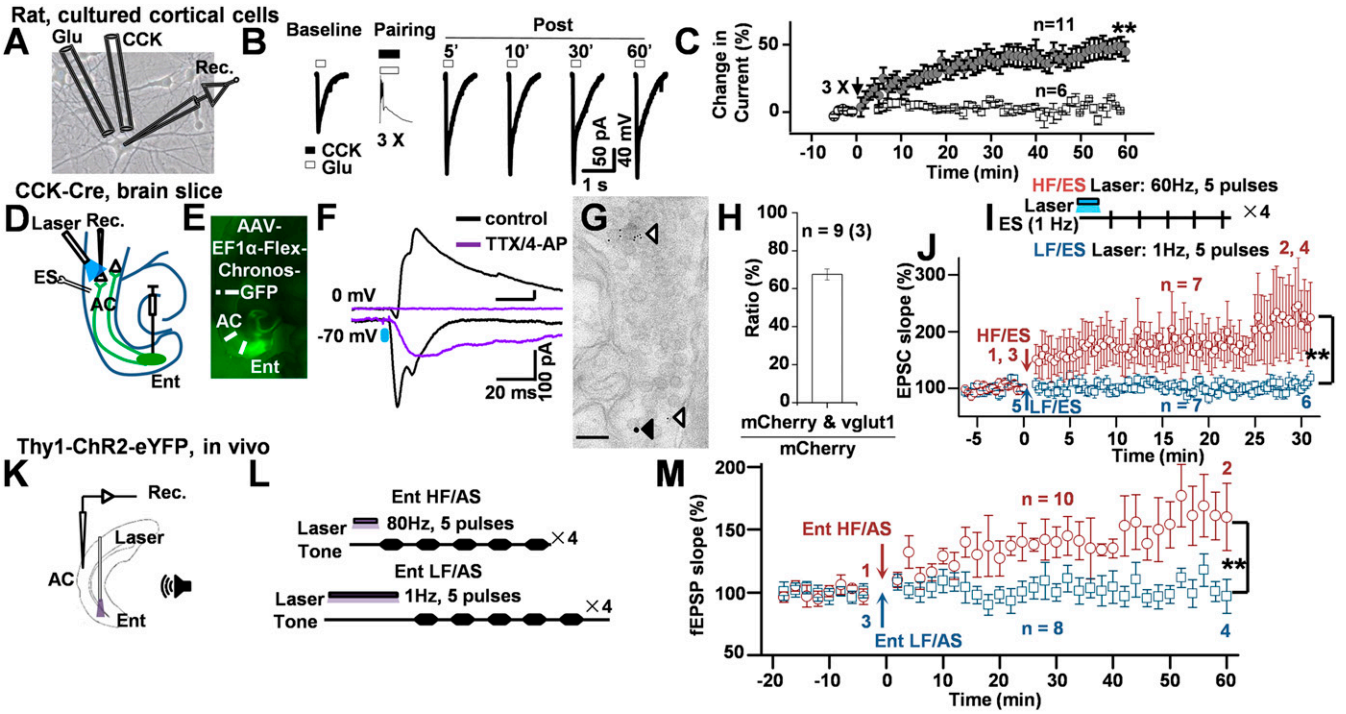

Fig. 3. CCK puffing or stimulation of entorhino-neocortical projections induced LTP in cultured cells, brain slices, and in vivo preparation. (*A*) Experimental set-up. A cultured neuron was whole-cell–clamped and two pipettes, one for Glu puffing and another for CCK puffing, were placed near the recorded neuron. (Magnification, 20×.) (*B*) Glutamate-activated current responses are shown before (baseline) and at 5, 10, 30, and 60 min after the pairing. CCK was repeatedly puffed simultaneously with glutamate three times during the pairing. (*C*) The time course of the change of the group data are shown before (open circle) and after (filled circle) the pairing, together with the control group with no pairing (no CCK puffing, no glutamate puffing, and no depolarization of the neurons, square) (two-way RM ANOVA, $^{**}P < 0.001$). (*D*) Positions of the whole-cell recording pipette, electrical stimulation electrode, and the optical fiber in a slice of CCK-Cre mice with AAV-Ef1α-Flex-Chronos-GFP injected in Ent. (*E*) A photo shows the virus injection site (Ent) and recording site (AC). (*F*) Voltage-clamp recordings to laser stimulation (blue) (*Upper*: holding potential, 0 mV; *Lower*: holding potential, −70 mV; room temperature) under control situation (black) and when incubated with TTX and 4-AP (purple). (*G*) Immuno-electron microscopy shows the colocalization of vglut1 and the cortical projection terminals of the entorhinal CCK neurons. Gold-particles of 15 nm show the immunoreactivities to mCherry (closed arrowheads), while those of 6 nm show the immunoreactivities to vglut1 (open triangles). AAV-EF1α-DIO-mCherry was injected in the entorhinal cortex of CCK-Cre mouse. (Scale bar, 100 nm.) (*H*) The ratio of mCherry$^+$ terminals that contain vglut1 over all mCherry$^+$ terminals. (*I*) HF/ES and LF/ES pairing protocol in which 60 Hz (HF) or 1 Hz (LF) laser stimulation at the auditory cortex was followed by 1 Hz ES. (*J*) Normalized slopes of EPSCs in response to the electrical stimulation before and after the HF/ES (red circle) or LF/ES (blue square) stimulation protocols (two-way RM ANOVA, $^{*}P < 0.001$). (*K*) Positions of the recording electrode in the auditory cortex and laser fiber in the entorhinal cortex of Thy1-Chr2-eYFP mice. (*L*) Ent HF/AS and Ent LF/AS protocols in which high frequency or low-frequency laser stimulation of the entorhinal cortex was followed by presentations of an auditory stimulus. (*M*) Normalized slopes of fEPSPs in response to the auditory stimulus before and after the Ent HF/AS (red circle) or Ent LF/AS (blue square) stimulation protocols (two-way RM ANOVA, $^{**}P < 0.001$). Data are expressed as mean ± SEM. Ent, entorhinal cortex; Ent HF/AS, high-frequency laser stimulation at entorhinal cortex paired with auditory stimuli; Ent LF/AS, low-frequency laser stimulation at entorhinal cortex paired with auditory stimuli; Glu, glutamate; HF/ES, high-frequency laser stimulation paired with electrical stimulation; LF/ES, low-frequency laser stimulation paired with electrical stimulation; TTX/4-AP, tetrodotoxin/4-Aminopyridine.

cortical LTP and the activation of the entorhino-neocortical CCK projections with patch-clamp recording on auditory neurons in the brain slice. Although the CCK mRNA levels of the CCK-Cre mice are 64% lower than in wild-type mice, we expected that the partial CCK production from their entorhinal neurons is still enough to induce neuroplasticity. CCK-Cre mice were injected with AAV-Ef1α-Flex-Chronos-GFP in the entorhinal cortex at 6 wk before the preparation of slices (Fig. 3 *D* and *E*). AAV-Ef1α-Flex-Chronos-GFP is a Cre-dependent virus that transfects any neuron in the injected area and leads to Chronos-GFP expression only in the Cre-expressing neurons. We targeted the excitatory neurons (*SI Appendix*, Fig. S10*A*). Laser activation of the AAV-infected terminals in the auditory cortex evoked both excitatory postsynaptic currents (EPSCs, with voltage clamped at −70 mV) and inhibitory postsynaptic currents (IPSCs, with voltage clamped at 0 mV) from the patched neurons (Fig. 3*F*, black curves). When action potentials of neurons in the slice were blocked by application of TTX/4-AP, only EPSCs were evoked by the laser stimulation, indicating that those monosynaptic projections from the entorhinal cortex to the auditory cortex were excitatory (Fig. 3*F*, purple curves). It was also obvious that the latency of EPSC was much shorter than that of IPSC, although the amplitude was opposite (*SI Appendix*, Fig. S10 *B–D*). Our electron microscopy images confirmed that most entorhino-neocortical projection CCK neurons were glutamatergic neurons (Fig. 3 *G* and *H*) [67.5 ± 2.9% mCherry$^+$ terminals are vesicular glutamate transporter 1 positive (vglut1$^+$), nine subfields from three mice].

HFS induces the release of CCK in the auditory cortex (Fig. 1 *E* and *F*), and the entorhino-neocortical projections are CCK$^+$ (18). Here, we investigated whether pairing HF laser activation of those entorhino-neocortical terminals (five pulses at 60 Hz) with the electrical stimulation of the auditory cortex (ES at 1 Hz; HF/ES) could induce neocortical LTP in the auditory cortex (see preparation in Fig. 3*D* and pairing paradigm in Fig. 3*I*). We presumed that HF laser stimulation induces the release of CCK, and the ES evokes pre- and postsynaptic activation. As a control, we used low-frequency laser stimulation (five pulses at 1 Hz) paired with ES (1 Hz; LF/ES). This stimulation protocol was repeated four times at 10-s intervals. With the AAV-Ef1α-Flex-Chronos-GFP, the entorhino-neocortical terminals were activated by HF laser at 60 Hz and 80 Hz (*SI Appendix*, Fig. S10 *E* and *F*) and patched neurons showed reliable EPSC to each laser pulse of the burst. The EPSC slope of patched neurons increased to 221.0 ± 12.2% at the end of 30 min after the HF/ES, but not to the LF/ES [two-way RM ANOVA, significant interaction $F(1, 208) = 44.9$, $P < 0.001$; pairwise comparison, before vs. after HF/ES, $P < 0.001$, $n = 7$; pairwise comparison, before vs. after LF/ES, $P = 0.85$, $n = 7$] (Fig. 3*J* and *SI Appendix*, Fig. S10*G*). Interestingly, the EPSC of two neurons in the HF/ES group started to show the spike currents at 25 min postpairing (one example is showed in *SI Appendix*, Fig. S10*G*, 3-4). These results indicate that HF activation of entorhino-neocortical terminals followed by electrical stimulation of the cortex induces cortical LTP.

Entorhinal HFS induces in Vivo Neocortical LTP in fEPSP to the Natural Stimulus. HFS induces the release of CCK in the auditory cortex (Fig. 1 *E* and *F*); thus, we surmised that pairing a natural auditory stimulus (presynaptic activation) after HF activation of the entorhinal cortex would potentiate the neuronal response to the natural auditory stimulus. We implanted an optical fiber in the entorhinal cortex and recording electrodes in the auditory cortex of Thy1-ChR2-eYFP mice (Fig. 3*K*). Neuronal spike activities or field potentials were recorded from electrodes implanted in the entorhinal cortex and the auditory cortex. HF (five pulses at 80 Hz; Ent HF) or LF (five pulses at 1 Hz; Ent LF) laser stimulation of the entorhinal cortex was followed by five presentations of an auditory stimulus at 1 Hz; this stimulation protocol was repeated four times at 10-s intervals (Fig. 3*L*). Entorhinal neurons responded to HF laser stimulation of up to 80 Hz with spikes (*SI Appendix*, Fig. S11*A*), and auditory cortical neurons responded to entorhinal HF laser stimulation with excitatory field potentials (*SI Appendix*, Fig. S11*B*). Neuronal responses to the auditory stimulus were recorded for 16 min before and 60 min after the auditory stimulation (AS) protocol. We observed that the HF protocol (Ent HF/AS) [two-way RM ANOVA, significant interaction $F(1, 88) = 20.9$, $P < 0.001$; pairwise comparison, before vs. after Ent HF/AS, $P < 0.001$, $n = 10$ recordings from nine mice], but not the LF protocol (Ent LF/AS) induced LTP to the auditory stimulus (pairwise comparison, before vs. after Ent LF/AS, $P = 0.50$, $n = 8$ recordings from seven mice) (Fig. 3*M* and *SI Appendix*, Fig. S11*C*). The results confirmed that projections from the entorhinal cortex are important for neocortical LTP induction and that burst-firing of entorhinal neurons may be the key to triggering CCK release and inducing LTP in the auditory cortex.

Entorhinal Projections Enable Neocortical LTP and Associative Memory. As mentioned in the Introduction, we focused on the entorhino-neocortical projection CCK$^+$ neurons in the present study, although there are many different types of CCK$^+$ neurons. In the next experiment, we induced entorhinal CCK-enabled LTP of the auditory responses in the auditory cortex and demonstrated that the formation of this LTP led to a behavioral change (i.e., freezing). To obtain direct evidence that HFS of the entorhino-neocortical projections enables the potentiation of neuronal responses and associative memory formation in the auditory cortex, we conducted experiments that allowed for direct optogenetic manipulation of specific projection neurons by injecting Cre-dependent AAV-EF1α-DIO-hChR2(E123T/T159C)-eYFP into the entorhinal cortex of CCK-Cre mice and adopting CCK$^{-/-}$(CCK-CreER) mice as the control group (Fig. 4 and *SI Appendix*, Fig. S12).

In the first experiment, we tested whether cortical LTP induction via HFS of entorhino-neocortical projections occurs in the above AAV-injected CCK-Cre mice (Fig. 4*A*). Entorhinal neurons transfected with the virus projected to neocortical areas, including the auditory cortex (Fig. 4*B*). We found that the majority of the transfected CCK neurons in the entorhinal cortex were glutamatergic neurons [76.6% of CCK neurons (red) expressed CamKII (green) in Fig. 4*B*]. At least 6 wk after virus injection into the entorhinal cortex, recording/stimulating electrodes and optical fibers were implanted in the auditory cortex of CCK-Cre mice (Fig. 4*C*). We observed that neurons in the auditory cortex responded to single pulses or a burst (80 Hz) of laser stimulation with excitatory field potentials (Fig. 4*D*). Next, we used a similar pairing protocol as employed in the previous experiment (Fig. 3*L*), but with additional electrical stimulation presented at 50 ms after the onset of each tone stimulus (Fig. 4*E*). The single-pulse electrical stimulation of the auditory cortex was used as a cue in the following behavioral test. The auditory cortical neurons showed potentiated responses to the auditory stimulus after the HF/AS/ES protocol [two-way RM ANOVA with a Greenhouse–Geisser correction, significant interaction $F(1.8, 162.7) = 20.2$, $P < 0.001$; pairwise comparison, before vs. after first HF/AS/ES, $P < 0.001$; after first vs. second HF/AS/ES, $P = 0.32$, $n = 10$ from 10 mice] (Fig. 4 *F* and *G*), but not after the LF/AS/ES protocol (pairwise comparison, before vs. after first LF/AS/ES, $P = 1$; after first vs. second LF/AS/ES, $P = 1$, $n = 8$ from 8 mice). Despite relatively short monitoring of the changes in neuronal responses (15 min after the first pairing and another 15 min after the second pairing), the pattern of potentiation resembled that observed after the entorhinal HF/AS protocol in Fig. 3*M*. Representative multiunit activities in points 1, 2, and 3 for the HF/AS/ES condition, and in 4, 5, and 6 for the LF/AS/ES condition are shown in Fig. 4*H*.

Our subsequent experiments aimed to confirm whether LTP induced by HFS of the CCK entorhino-neocortical projections in the auditory cortex was generated by the release of CCK. We found that vehicle infusion (ACSF) before HF/AS/ES induced LTP, while an infusion of a CCKBR antagonist (L365,260) before HF/AS/ES

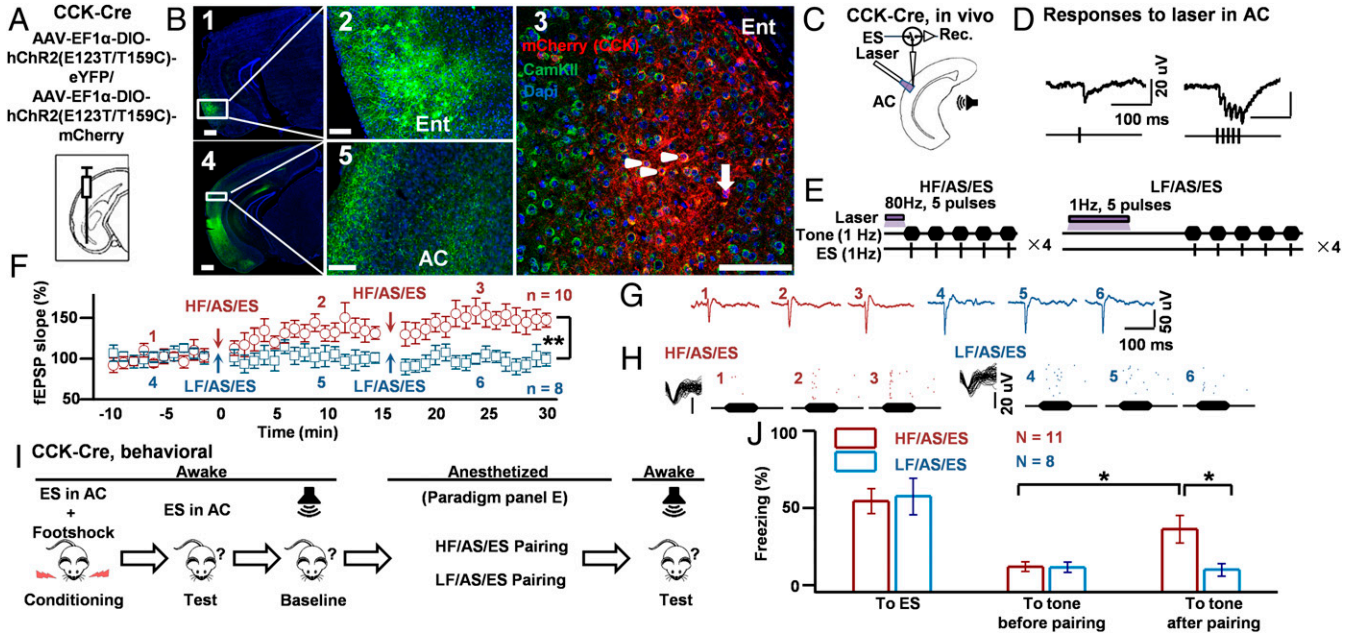

Fig. 4. HFS of CCK-containing entorhino-neocortical projections enables the association between an auditory stimulus and electrical stimulation of the auditory cortex, leading to behavioral changes. (*A*) AAV-EF1α-DIO-hChR2(E123T/T159C)-eYFP (for B1, 2, 4, and 5) or AAV-EF1α-DIO-hChR2(E123T/T159C)-mCherry (for B3) was injected into the entorhinal cortex of CCK-Cre mice. (*B*) Images of virus expression in the entorhinal cortex (1–3) and the auditory cortex (4, 5). (Scale bars: 500 μm for 1 and 4; 100 μm for 2, 3, and 5.) In 3, mCherry (CCK), CamKII, and DAPI were overlapped (Arrowhead: neurons express both CamkII and CCK; arrow: a neuron only expresses CCK). (*C*) Positions of the laser fiber and stimulating/recording electrodes in the auditory cortex of CCK-Cre mice injected with AAV-EF1α-DIO-hChR2(E123T/T159C)-eYFP in the entorhinal cortex. (*D*) fEPSP responses to laser stimulation (*Upper*: 1 Hz; *Lower*: 80 Hz) in the auditory cortex. (*E*) HF/AS/ES and LF/AS/ES pairing protocols. (*F*) Normalized slopes of fEPSPs after the HF/AS/ES (red circle) or LF/AS/ES (blue square) pairing protocols (two-way RM ANOVA, $^{**}P < 0.001$). (*G*) Representative single fEPSP traces before and after the HF/AS/ES (1–3) and LF/AS/ES (4–6) protocols. (*H*) Unit responses to the auditory stimulus before and after the pairings of HF/AS/ES (1–3) and LF/AS/ES (4–6). (*I*) Cued fear conditioning and pairing protocols. (*J*) Freezing percentages in response to the paired auditory stimulus before and after the HF/AS/ES (Red) or LF/AS/ES (Blue) pairing (two-way RM ANOVA, $^{*}P < 0.05$). Data are expressed as mean ± SEM. HF/ES/AS, high-frequency laser stimulation paired with electrical stimulation and auditory stimuli; LF/ES/AS, low-frequency laser stimulation paired with electrical stimulation and auditory stimuli.

failed to induce LTP in the auditory cortex of CCK-Cre mice (*SI Appendix*, Fig. S12 *B* and *C*). An additional control experiment was carried out on $CCK^{-/-}$ mice, adopting the same protocol that was used in the CCK-Cre mice. Results showed that no potentiation was induced after the HF/AS/ES protocol (*SI Appendix*, Fig. S12 *D* and *E*), suggesting that the loss of LTP induction in $CCK^{-/-}$ mice was generated by the absence of CCK release.

We next examined whether the LTP induced by HF/AS/ES pairing in the anesthetized mouse could be demonstrated in a behavioral context. We paired electrical stimulation of the auditory cortex with the footshock for 5 d until the mice showed stable freezing responses to the conditioned single-pulse electrical stimulation of the auditory cortex in the absence of footshock (Fig. 4 *I* and *J*, "to ES"). An auditory stimulus that triggered no freezing response and evoked weak neuronal responses was then selected as the pairing auditory stimulus for each mouse. Similar to the experiments conducted above, pairings of either HF/AS/ES or LF/AS/ES were employed while mice were in anesthetized conditions. The neurons that showed potentiated responses to the auditory stimulus after HF/AS/ES pairing were presumed to overlap with those activated by the electrical stimulation of the auditory cortex. Therefore, we expected that the paired auditory stimulus would induce freezing behavior by activating those neurons. Indeed, mice in the HF/AS/ES group showed more freezing in response to the auditory stimulus after pairing than before pairing [two-way RM ANOVA, significant interaction $F(2, 34) = 4.1$, $P = 0.026$; pairwise comparison, before vs. after HF/AS/ES pairing $P = 0.003$, $n = 11$ mice] (Fig. 4*J*), whereas mice in the LF/AS/ES group showed no change in freezing after pairing (pairwise comparison, $P = 1$, $n = 8$ mice). Mice in the HF/AS/ES group also showed more freezing than mice in the LF/AS/ES group after pairing (36.4 ± 6.8% vs. 10.0 ± 8%, pairwise comparison, $P = 0.022$).

To further verify these findings, we conducted a parallel experiment that included injecting AAV-CaMKIIa-hChR2 (E123T/T159C)-mCherry into the entorhinal cortex of C57 mice. The experiment on wild-type mice circumvented the pitfall of the lower CCK mRNA level in the entorhinal cortex of the CCK-Cre mice. Of note, the virus did not selectively infect CCK^{+} neurons. Results emulated those above, wherein the HF/AS/ES group showed more freezing than the LF/AS/ES group (*SI Appendix*, Fig. S13). Both experiments demonstrated that an association between an auditory stimulus and electrical stimulation of the auditory cortex, reflected by potentiated neuronal responses to the auditory stimulus, could be established while mice were under anesthesia. Moreover, conditioning the electrical stimulation of the auditory cortex to the footshock caused mice to exhibit freezing in response to the auditory stimulus, providing further evidence of an association between the auditory stimulus and electrical stimulation of the auditory cortex. Therefore, HFS of CCK-containing entorhino-neocortical projections appears to be a pivotal contributor to neocortical neuroplasticity and associative memory formation.

Either the CCKBR or NMDAR Antagonist Blocks HFS-Induced LTP. HFS induced neocortical LTP is largely thought to be NMDAR-dependent. The above results demonstrate that HFS-induced neocortical LTP is CCK-dependent. A natural question to ask is: What is the relationship between the NMDAR and CCK in neocortical LTP induction? To establish a physiological correlation

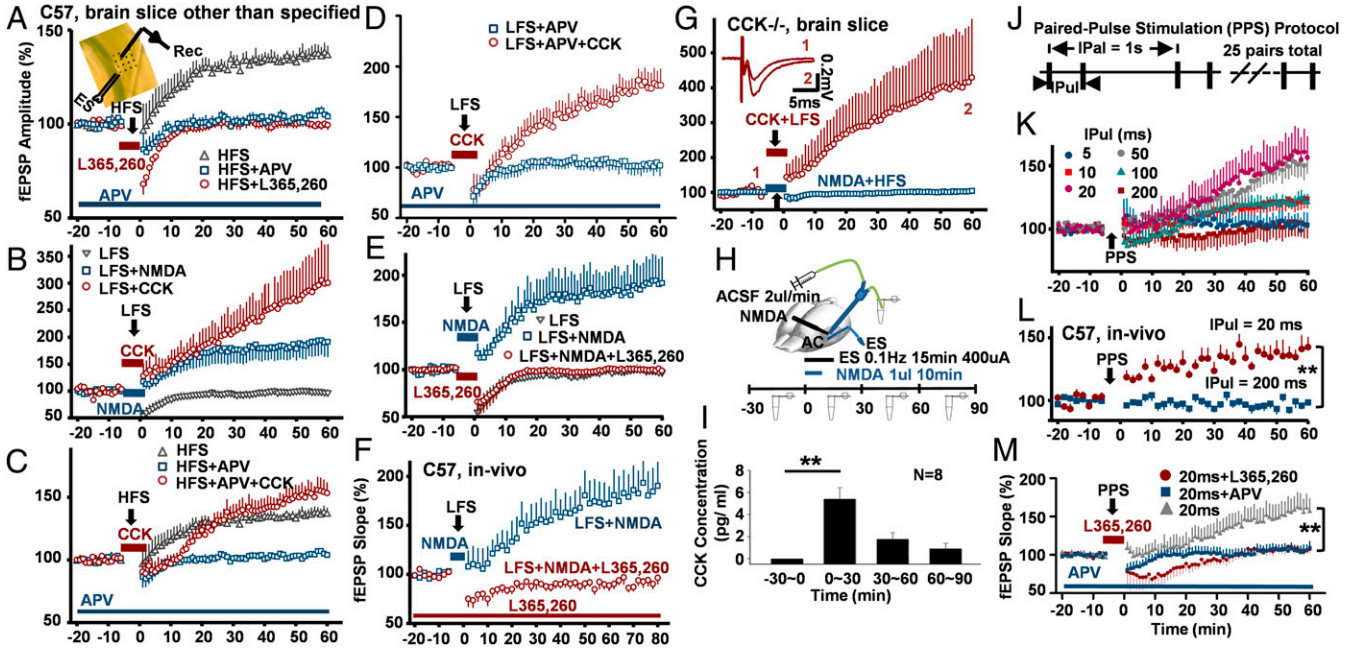

Fig. 5. NMDARs control the release of CCK, which in turn enables CCK-dependent neocortical LTP. (*A*) Either an NMDAR antagonist or CCKBR antagonist blocked HFS-induced LTP in C57 cortical slices. APV was applied throughout all of the recording period, while L365,260 was applied after the baseline recording, but before the HFS. *Inset* shows positions of recording and electrical stimulating sites. (*B*) Coupled with LFS, both NMDA and CCK induced LTP in C57 cortical slices. (*C*) Blocking of NMDARs did not block LTP in the presence of CCK in C57 cortical slices with HFS. (*D*) Blocking of NMDARs did not block LTP in the presence of CCK in C57 cortical slices with LFS. (*E*) NMDA induced LTP was blocked by application of CCKBR antagonist L365,260 in the C57 slices. (*F*) NMDA induced LTP was blocked by application of CCKBR antagonist, L365,260, in the auditory cortex of anesthetized C57 mice. L365,260 or control (DMSO+ACSF) was infused during the whole experiment. (*G*) No LTP was induced by NMDA application, but a marked induction of LTP was generated by CCK application in the cortical slices of $CCK^{-/-}$ mice. *Inset* shows representative single fEPSP traces before and after the CCK+LFS (1, 2). (*H*) Diagram illustrating injecting cannula for NMDA (100 μM, 1 μL) application and microdialysis with a schedule showing time points of ACSF collection and NMDA application. (*I*) Local application of NMDA triggered CCK release in the auditory cortex of C57 mice. (*J–M*) A new paradigm for LTP induction: a 25 PPS protocol. (*J*) Twenty-five pairs of paired-pulses with varied IPul between 5 ms and 200 ms and fixed IPal of 1 s. (*K*) The induction of LTP with different IPuls. (*L*) LTP was induced by the PPS protocol when IPul was 20 ms, but not 200 ms in the auditory cortex of anesthetized C57 mice (two-way RM ANOVA, $^{**}P < 0.001$). (*M*) LTP induced with the PPS protocol was blocked by infusion of either APV or L365,260 (two-way RM ANOVA, $^{**}P < 0.001$). Data are expressed as mean ± SEM.

between NMDAR- and CCK-associated LTP, we conducted in vitro electrophysiological recordings with a four-slice multielectrode array system in cortical slices from C57 mice. We began by using HFS in conjunction with common antagonists for both NMDAR and CCKBR [i.e., DL-2-amino-5-phosphonovaleric acid (APV, 100 μM) and L365,260, respectively]. We found that HFS-induced LTP in cortical slices of C57 mice was almost fully blocked by the NMDAR antagonist and fully blocked by the CCKBR antagonist [two-way RM ANOVA, significant interaction $F(2, 207) = 306.2$, $P < 0.001$; increased by 35.8 ± 1.1%, pairwise comparison, before vs. after the HFS, $P < 0.001$, $n = 7$; changed by 4.4 ± 1.1%, pairwise comparison, before vs. after the HFS with APV, $P < 0.001$, $n = 7$; changed by 0.3 ± 1.1%, pairwise comparison, before vs. after the HFS with L365,260, $P = 0.79$, $n = 7$] (Fig. 5*A*).

LFS in the Presence of CCK or NMDA Induces LTP. Normally, LFS does not induce LTP in cortical slices, as represented in fEPSP. Our initial recordings reaffirmed this (Fig. 5*B*). However, infusion of either NMDA or CCK in conjunction with LFS for 5 min produced significant LTP [two-way RM ANOVA, significant interaction $F(2, 197) = 53.0$, $P < 0.001$; changed by −1.0 ± 13.7%, pairwise comparison, before vs. after the LFS, $P = 0.94$, $n = 6$; increased by 89.1 ± 12.7%, pairwise comparison, before vs. after the LFS with NMDA, $P < 0.001$, $n = 7$; markedly increased by 191.1 ± 12.7%, pairwise comparison, before vs. after the LFS with CCK, $P < 0.001$, $n = 7$] (Fig. 5*B*).

NMDAR-Dependent LTP Fully Blocked by the CCKBR Antagonist. Application of both CCK and NMDA induced a significant LTP even after LFS. In the next experiment, we examined the relationship between the CCK and NMDAR signaling pathways, asking which is upstream and which is downstream. Our first assumption was that the CCK signal pathway is upstream. If true, LTP cannot be induced, with or without CCK application, when NMDARs are blocked by APV. Surprisingly, we found that induction of LTP was generated by CCK even after blockade of NMDARs both with HFS [two-way RM ANOVA, significant interaction $F(2, 197) = 158.5$, $P < 0.001$; increased by 35.8 ± 1.9%, pairwise comparison, before vs. after the HFS, $P < 0.001$, $n = 7$; changed by 4.4 ± 1.9%, pairwise comparison, before vs. after the HFS with APV, $P = 0.021$, $n = 7$; significant increase by 52.3 ± 2.0%, pairwise comparison, before vs. after the HFS with APV and CCK, $P < 0.001$, $n = 6$] (Fig. 5*C*) and LFS [two-way RM ANOVA, significant interaction $F(1, 188) = 248.6$, $P < 0.001$; changed by 2.6 ± 3.3%, pairwise comparison, before vs. after the LFS with APV, $P = 0.45$, $n = 10$; significant increase by 79.1 ± 3.5%, pairwise comparison, before vs. after the LFS with APV and CCK, $P < 0.001$, $n = 9$] (Fig. 5*D*), rejecting the above hypothesis. In other words, CCK is in the downstream of the NMDAR pathway. We then assumed that NMDARs are critical for release of CCK and that a CCKBR antagonist would prevent NMDAR-associative LTP. In fact, coapplication of NMDA and L365,260 completely blocked LTP induced by LFS/NMDA [two-way RM ANOVA, significant interaction $F(2, 197) = 132.4$, $P < 0.001$; changed by −1.0 ± 4.8%, pairwise comparison, before vs. after the LFS, $P = 0.83$, $n = 6$; increased by 89.1 ± 4.5%, pairwise comparison, before vs. after the LFS with NMDA, $P < 0.001$, $n = 7$; changed by −0.5 ± 4.5%, pairwise comparison, before vs. after

the LFS with NMDA and L3652,60, $P = 0.90$, $n = 7$] (Fig. 5*E*). We repeated this critical experiment in the auditory cortex of anesthetized mice and found, again, that NMDAR-induced LTP was blocked when coapplied with L365,260 [two-way RM ANOVA, significant interaction $F(1, 108) = 89.9$, $P < 0.001$; significant increase by 72.2 ± 6.4%, pairwise comparison, before vs. after the LFS with NMDA, $P < 0.001$, $n = 10$; changed by −10.1 ± 5.9%, pairwise comparison, before vs. after the LFS with NMDA and L365,260, $P = 0.088$, $n = 12$] (Fig. 5*F*).

No Rescuing Effect Produced by NMDA Application on LTP and Cue–Cue Association in CCK$^{-/-}$ Mice. The earlier in vivo experiment showed that local application of CCK induced LTP in the auditory cortex of CCK$^{-/-}$ mice. Similarly, we found that in cortical slices of CCK$^{-/-}$ mice, application of CCK lead to LTP (Fig. 5*G* and *SI Appendix*, Fig. S15). However, NMDA application with pairing of HFS in cortical slices of CCK$^{-/-}$ mice failed to produce LTP [two-way RM ANOVA, significant interaction $F(1,148) = 52.7$, $P < 0.001$; significant increase by 304.1 ± 30.5%, pairwise comparison, before vs. after the LFS with CCK, $P < 0.001$, $n = 7$; changed by 1.4 ± 28.5%, pairwise comparison, before vs. after the LFS with NMDA, $P = 0.96$, $n = 8$] (Fig. 5*G*). In the earlier behavioral experiment on CCK$^{-/-}$ mice, the tone–tone association was not improved after intravenous infusion of NMDA (*SI Appendix*, Fig. S5 *D* and *E*). These results indicate that NMDARs are not acting in the downstream of the CCK receptor in LTP induction, rather the activation of NMDARs are likely triggering CCK release. Taken together, this implies that LTP induction stems from the NMDAR-mediated release of CCK. To advance this hypothesis, we investigated the mechanisms of CCK release.

CCK Release Controlled by NMDARs. We used microdialysis and ELISA to establish that local application of NMDA induced the CCK release in the neocortex (Fig. 5*H*). The CCK concentration in the dialyzed CSF increased significantly from 0 (undetectable level) to 5.4 ± 1.0 pg/mL [one-way RM ANOVA, $F(3, 21) = 15.6$, $P < 0.001$; pairwise comparison, before vs. first 30 min after NMDA application, $P = 0.008$, $n = 8$], and returned to 1.8 ± 0.6 pg/mL in the following 30 min and 0.9 ± 0.5 pg/mL in between 60 and 90 min (Fig. 5*I*).

Paired-Pulse Stimulation Protocol Instead of HFS Protocol to Induce NMDAR-Dependent LTP. One difference between the HFS and LFS stems from the interval between two consecutive pulses: one is short and the other one is long. We hypothesized that the first pulse activates the glutamatergic CCK terminal to release glutamate that then activates the NMDARs, whereby the activated NMDARs induce CCK release, if the second pulse arrives within the critical interval. To examine this hypothesis, we employed a new stimulation protocol to replace the HFS protocol for LTP induction: 25 pulse-pairs (interpair-interval, IPaI = 1 s; interpulse-interval within the pulse-pair, IPuI, varied from 5 to 200 ms) (Fig. 5*J*). Interestingly, the paired-pulse stimulation (PPS) protocol of IPuI between 10 and 100 ms induced LTP, while that of IPuI of 5 ms and 200 ms did not [two-way RM ANOVA, significant interaction $F(5, 434) = 41.4$, $P < 0.001$; changed by 2.6 ± 3.9%, pairwise comparison, before vs. after the PPS with IPuI = 5 ms, $P = 0.50$, $n = 6$; slightly increased by 21.4 ± 3.6%, pairwise comparison, IPuI = 10 ms, $P < 0.001$, $n = 7$; increased by 56.9 ± 3.4%, pairwise comparison, IPuI = 20 ms, $P < 0.001$, $n = 8$; increased by 50.1 ± 3.6%, pairwise comparison, IPuI = 50 ms, $P < 0.001$, $n = 7$; slightly increased by 20.6 ± 3.4%, pairwise comparison, IPuI = 100 ms, $P < 0.001$, $n = 8$; changed by 4.2 ± 3.4, pairwise comparison, IPuI = 200 ms, $P = 0.22$, $n = 8$] (Fig. 5*K* and *SI Appendix*, Fig. S16).

We performed an in vivo experiment to further confirm LTP induction with the PPS protocol and found that PPS of IPuI of 20 ms induced LTP in the auditory cortex of anesthetized mice, while the IPuI of 200 ms did not [two-way RM ANOVA, significant interaction $F(1, 103) = 67.3$, $P < 0.001$; significant increase by 35.9 ± 3.2%, pairwise comparison, before vs. after the PPS with IPuI = 20 ms, $P < 0.001$, $n = 6$; changed by 2.2 ± 3.4%, pairwise comparison, before vs. after the PPS with IPuI = 200 ms, $P = 0.52$, $n = 10$] (Fig. 5*L*). A PPS of 20–50 Hz means an optimal time interval between 20 and 50 ms. Next, in efforts to reveal how the required initial stimulation of NMDARs may affect CCK release, we applied APV during the PPS. This completely blocked the potentiation [two-way RM ANOVA, significant interaction $F(2, 217) = 56.2$, $P < 0.001$; changed by 6.6 ± 4.0%, pairwise comparison, before vs. after the PPS with APV, $P = 0.10$, $n = 7$] (Fig. 5*M*). Similarly, application of the CCKBR antagonist (L365,260) blocked the potentiation (changed by 8.0 ± 4.0%, pairwise comparison, before vs. after the PPS with L365,260, $P = 0.047$, $n = 7$) (Fig. 5*M*).

We can assume that the first action potential would induce glutamate release, which in turn activates NMDARs creating the conditions necessary for CCK release. The results imply that the critical interval for the second action potential to release CCK from the terminal falls between 10 and 100 ms. Our proposed mechanism also explains why LTP could be induced with LFS, when NMDA was applied each pulse of LFS can trigger the release of CCK, enabling the induction of LTP and the coapplication of CCKBR antagonist prevents this LTP induction. In sum, the conjoint electrophysiological data strongly suggested an interaction between NMDARs and CCK in LTP induction (Fig. 6).

Discussion

In the present study, we have provided substantial evidence supporting the hypothesis that CCK plays an integral role in HFS-induced LTP in the neocortex and the encoding of auditory associative memory. First, our in vivo experiments show that: (*i*) HFS induces release of CCK in the auditory cortex; (*ii*) HFS-induced

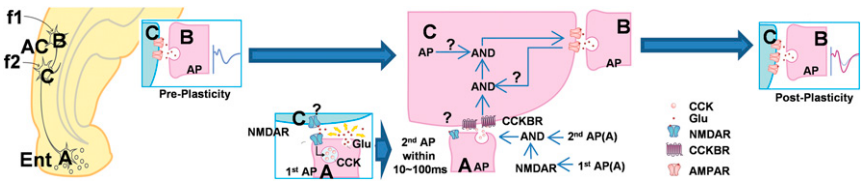

Fig. 6. A schematic illustration shows that CCK release triggered by either/both pre- or/and postsynaptic NMDA receptors produces LTP and sound–sound associative memory. CCK released from the entorhinal CCK neuron (Ent, neuron A) that projects to the auditory cortex enhances the connectivity of two neurons in the auditory cortex (neuron B to neuron C) (*Left* part). When the first action potential comes to neuron A, glutamate is released from A and activates its own NMDAR on its terminal (*Lower Center, Left*). The NMDAR will enable the release of CCK from A, if the second action potential comes to the terminal of neuron A within a period of 10–100 ms (*Lower Center, Right*). Together with other conditions, such as activation of the B → C synapse and action potentials of neuron C, the released CCK from A that activates the CCKBR on neuron C enables neuroplasticity of B → C pathway, inducing potentiated EPSC for the B → C synapse (*Upper Center*).

neocortical LTP is blocked by a CCKBR antagonist; (*iii*) LTP is not induced by HFS in the neocortex of $CCK^{-/-}$ mice; (*iv*) LFS (0.1 Hz), together with direct CCK application, induces LTP in the neocortex of both $CCK^{-/-}$ and wild-type mice; and (*v*) $CCK^{-/-}$ mice and mice treated with the CCKBR antagonists show a marked deficit in the association of two tones in behavioral experiments. Second, in cultured cortical neurons, we showed that the glutamate-activated current is significantly potentiated after a three-trial pairing of the coapplication of CCK and glutamate and depolarization of the recorded neurons, suggesting that LTP can be induced by activation of postsynaptic CCK receptors. Third, that HFS of the entorhino-neocortical CCK projection can induce neocortical LTP was confirmed in a set of in vitro and in vivo experiments showing enhanced responses to electrical stimulation as well as to natural sound stimulus in the auditory cortex. Fourth, that HFS of the entorhino-neocortical CCK projection, but not LFS, is crucial for LTP induction in associative memory formation in the auditory cortex is evidenced by combining various methodologies, such as optogenetics, electrophysiology, and behavioral tests.

Importantly, our results suggested that CCK acts downstream of the NMDAR pathway. In support of this, we found that: (*i*) either the CCKBR or NMDAR antagonist blocks HFS-induced LTP, and (*ii*) LFS induces LTP in the presence of either CCK or NMDA. Moreover, LTP is induced upon application of CCK even when NMDARs are blocked, while application of the CCKBR antagonist completely blocks LTP induced by LFS/NMDA. Finally, microdialysis experiments show that NMDARs control the release of CCK, and the PPS protocol, instead of the HFS protocol, successfully induces NMDAR-dependent LTP which can be blocked by CCKBR antagonist.

HFS-Induced Cortical LTP Is CCK Dependent. LTP, which was discovered in the hippocampus over 40 y ago (3), has generally been regarded as the synaptic basis of learning and memory in vertebrates (4) (but contrary evidence also exists, e.g., ref. 31). Indeed, a recent study that selectively manipulated synapses with HFS and LFS successfully demonstrated that LTP was linked with associative memory (5). Our results complement those of recent studies using optogenetics to examine how neuronal assemblies support memories (5, 32, 33). We found that LTP in the rat and mouse auditory cortex could be induced by HFS of the auditory cortex, CCK infusion, or HFS of entorhino-neocortical projections. Together, our results lead us to conclude that HFS causes entorhinal projection neurons to release CCK into the auditory cortex, thereby inducing LTP in the auditory cortex in response to the auditory stimulus or electrical stimulation.

In additional experiments, we dissected the different components of neocortical LTP induction. Using patch-clamp recordings on cultured cortical neurons, we concluded that in the presence of CCK, LTP could be produced postsynaptically with just a few pairings of the pre- and postsynaptic activities. LTP was induced by CCK infusion into the auditory cortex without HFS, while no LTP could be induced in $CCK^{-/-}$ mice or in the presence of a CCKBR antagonist. Based on the hypothesis that HFS induces CCK release in the cortex, we tested whether the potentiation of neuronal responses occurs only for HF-stimulated inputs. After HFS of the entorhinal cortex, we observed LTP in response to an auditory probe stimulus presented at low-frequency. These results imply that LTP also occurs for non-HF–stimulated inputs, extending our current understanding beyond the idea that LTP only occurs for HF-stimulated inputs (34, 35). Furthermore, HFS of CCK-containing entorhino-neocortical terminals before the pairing of auditory and low-frequency electrical stimuli induced LTP to the auditory stimulus, again indicating the importance of CCK in inducing neocortical LTP. Furthermore, when the electrical stimulation was conditioned to a footshock before the pairing, the auditory stimulus triggered freezing responses in mice, indicating that mice had formed an association between electrical and auditory stimuli that meaningfully affected behavior.

CCK Enables Cue–Cue Association in the Auditory Cortex. Consistent with previous findings that CCK is associated with learning and memory (20, 36–38), we found that $CCK^{-/-}$ mice showed deficits in associative memory formation and cued fear-conditioning tests. Previous studies also showed that long-range projecting GABAergic CCK neurons in the entorhinal cortex to the hippocampus (22, 24) and local GABAergic CCK neurons in the hippocampus (21) participate in the formation of long-term memory. Earlier studies indicated that many CCK neurons in the neocortex are excitatory (25, 26), and we focused on the entorhino-neocortical projection neurons in the present study. CCK-containing entorhinal neurons in CCK-Cre mice labeled with AAV-EF1a-DIO-eYFP projected all of the way to the auditory cortex and other neocortical areas. Laser stimulation of these terminals elicited fEPSPs in the auditory cortex, suggesting that they are glutamatergic neurons. Studies have revealed that the formation of paired visual associations or paired visuoauditory associations critically depends on the perirhinal and entorhinal cortex (39, 40). Our results suggest that memory enhancement by deep-brain stimulation of the entorhinal cortex (41) may be related to the activation of CCK-containing entorhinal neurons. Additional evidence for this stems from our findings that showed $CCK^{-/-}$ mice had marked deficits in associating two different tones. The same trial number of the pairing of the two tones in the $CCK^{-/-}$ mice was not able to achieve the association between the two tones. We are not sure whether tripling the pairing trials could produce the same association of the two tones, as the fear conditioning could. Adult $CCK^{-/-}$ mice show normal auditory responses in the auditory cortex (*SI Appendix*, Fig. S6). The establishment of the thalamocortical circuit starts at P2 (42), possibly before the CCK expression; the issue of how CCK participates in the experience-dependent thalamocortical neuroplasticity during the development should be subjected to future investigation. The AS/ES pairing after HF activation of the entorhino-neocortical CCK terminals established an artificial association between the auditory and electrical stimuli in the present study. Association of the artificial manipulation using electrical stimulation and natural stimulus suggests it lies within neuroengineering and therapeutic applications.

NMDARs Control the Release of CCK and Lead to the Formation of LTP. Previous studies have shown that NMDARs enable the formation of associative memory and precipitate LTP induction (2, 6–9, 12). Interestingly, cortical application of a CCKBR antagonist blocked the formation of the associative memory between two tones with different frequencies in the C57 mice. Moreover, $CCK^{-/-}$ mice exhibited deficits in the formation of the above association, and while infusing NMDA failed to rescue the formation of associative memory, intravenous infusion of CCK-4 proved effective in alleviating these deficits. These results thus imply that CCK acts as a switch for the formation of associative memory, and is seemingly more vital in this scenario than NMDARs. In our cortical slice experiments, the required conditions that generated LTP suggest that the activation of NMDARs controls the release of CCK, which enables plastic alterations in the postsynaptic neuron. The result that no rescuing effect produced by NMDA application on LTP in $CCK^{-/-}$ mice implies that LTP induction stems from the NMDAR-mediated release of CCK. Our brain slice experiments also unveiled that the role of theta burst stimulation/HFS in LTP induction can be replaced with paired-pulses with short intervals between the pulses within each pair. Concomitantly, the data suggest that the first pulse within the pair activates the glutamatergic CCK terminals to release glutamate that in turn activates

NMDARs, which then act as a temporal gate that controls CCK release. Evidence for this stems from data showing that CCK is released only when the second pulse arrives within a critical interval (10–100 ms) (see the model in Fig. 6).

Direct application of NMDA has been shown to induce LTD in field potential when in high concentration (20–50 μM) and no change in low concentration (10 μM) (43). In our study, we administered NMDA in a low concentration (10 μM), but followed with LFS at high intensity (75% of saturated current or 130 μA, whichever the greater). It is presumed that this LFS triggers the release of CCK when the NMDARs are activated and then induces LTP. The difference between the preparation of the previous study and ours may explain why no LTP could be induced by only NMDA administration before (43). These differential results support our hypothesis about how NMDARs control CCK releasing. The microdialysis and ELISA result of local application of NMDA triggering the release of CCK further strengthens the hypothesis.

In summary, evidence suggests that the NMDARs control the release of CCK (see representative schematic drawing in Fig. 6). This enables CCK-dependent neocortical LTP and the formation of cue–cue associative memory. One important note is that the CCK pathway from the entorhinal cortex (A → B) is different from the cue–cue associative pathway (B → C). To the best of our knowledge, this is a set of results showing a potential mechanism underpinning associative memory formation through neuropeptidergic modulation and entorhinal stimulation.

Materials and Methods

Sprague-Dawley rats (only male, 8–12 wk) and C57/BL/6 (C57), Thy1-ChR2-eYFP (C57 background), CCK-Cre [Cck$^{tm1.1(Cre)Zjh/J}$, C57 background; Jackson Laboratory], CCK-CreER [Cck$^{tm2.1(Cre/ERT2)Zjh/J}$, C57 background, Jackson Laboratory] mice (both male and female, 8–12 wk) were used for in vivo extracellular recordings, in vitro cultured cell recordings, in vitro brain slice recordings, behavioral experiments, and immunohistochemistry. All experimental procedures were approved by the Animal Subjects Ethics Sub-Committees of the City University of Hong Kong. Full methods can be found in *SI Appendix, Materials and Methods*.

ACKNOWLEDGMENTS. We thank Guoping Feng (Massachusetts Institute of Technology) and Minmin Luo (Chinese Institute for Brain Research, Beijing) for sharing of some transgenic mouse lines for our preliminary study; Eduardo Lau for administrative and technical assistance; Tomas Hökfelt (Karolinska Institutet), Richard Salvi (New York University at Buffalo), Kuanhong Wang (NIH), Robert Oswald (Cornell University), Bin Hu (University of Calgary), and Jun Xia (Hong Kong University of Science and Technology) for critical comments; and Colin Blakemore (University of London), and Longnian Lin (East China Normal University) for insightful discussion. This work was supported by Hong Kong Research Grants Council, Guangdong Science and Technology Foundation, Natural Science Foundation of China, and Health and Medical Research Fund, Innovation and Technology Fund (Grants C1014-15G, MRP/101/17X, 31571096, 31371114, 31671102, 31200852, 31171060, 03141196, 01121906, 561313M, 11101215M, 11166316M, 11102417M, 11101818M, 2014B050505016). We also thank the following charitable foundations for their generous support: the Charlie Lee Charitable Foundation, the Fong Shu Fook Tong Foundation, and the Croucher Foundation.

1. Kandel ER (2001) The molecular biology of memory storage: A dialogue between genes and synapses. *Science* 294:1030–1038.
2. Artola A, Singer W (1987) Long-term potentiation and NMDA receptors in rat visual cortex. *Nature* 330:649–652.
3. Lomo T (1971) Potentiation of monosynaptic EPSPs in the perforant path-dentate granule cell synapse. *Exp Brain Res* 12:46–63.
4. Bliss TV, Collingridge GL (1993) A synaptic model of memory: Long-term potentiation in the hippocampus. *Nature* 361:31–39.
5. Nabavi S, et al. (2014) Engineering a memory with LTD and LTP. *Nature* 511:348–352.
6. Morris RG, Anderson E, Lynch GS, Baudry M (1986) Selective impairment of learning and blockade of long-term potentiation by an N-methyl-D-aspartate receptor antagonist, AP5. *Nature* 319:774–776.
7. Sakimura K, et al. (1995) Reduced hippocampal LTP and spatial learning in mice lacking NMDA receptor epsilon 1 subunit. *Nature* 373:151–155.
8. Gardoni F, et al. (1998) Calcium/calmodulin-dependent protein kinase II is associated with NR2A/B subunits of NMDA receptor in postsynaptic densities. *J Neurochem* 71:1733–1741.
9. Lisman JE, Zhabotinsky AM (2001) A model of synaptic memory: A CaMKII/PP1 switch that potentiates transmission by organizing an AMPA receptor anchoring assembly. *Neuron* 31:191–201.
10. Bear MF, Kirkwood A (1993) Neocortical long-term potentiation. *Curr Opin Neurobiol* 3:197–202.
11. Shimizu E, Tang YP, Rampon C, Tsien JZ (2000) NMDA receptor-dependent synaptic reinforcement as a crucial process for memory consolidation. *Science* 290:1170–1174.
12. Nakazawa K, et al. (2002) Requirement for hippocampal CA3 NMDA receptors in associative memory recall. *Science* 297:211–218.
13. Canto CB, Wouterlood FG, Witter MP (2008) What does the anatomical organization of the entorhinal cortex tell us? *Neural Plast* 2008:381243.
14. Swanson LW, Köhler C (1986) Anatomical evidence for direct projections from the entorhinal area to the entire cortical mantle in the rat. *J Neurosci* 6:3010–3023.
15. Innis RB, Corrêa FM, Uhl GR, Schneider B, Snyder SH (1979) Cholecystokinin octapeptide-like immunoreactivity: Histochemical localization in rat brain. *Proc Natl Acad Sci USA* 76:521–525.
16. Greenwood RS, Godar SE, Reaves TA, Jr, Hayward JN (1981) Cholecystokinin in hippocampal pathways. *J Comp Neurol* 203:335–350.
17. Köhler C, Chan-Palay V (1982) The distribution of cholecystokinin-like immunoreactive neurons and nerve terminals in the retrohippocampal region in the rat and Guinea pig. *J Comp Neurol* 210:136–146.
18. Li X, et al. (2014) Cholecystokinin from the entorhinal cortex enables neural plasticity in the auditory cortex. *Cell Res* 24:307–330.
19. Rehfeld JF (1978) Immunochemical studies on cholecystokinin. II. Distribution and molecular heterogeneity in the central nervous system and small intestine of man and hog. *J Biol Chem* 253:4022–4030.
20. Lo CM, et al. (2008) Characterization of mice lacking the gene for cholecystokinin. *Am J Physiol Regul Integr Comp Physiol* 294:R803–R810.
21. Hefft S, Jonas P (2005) Asynchronous GABA release generates long-lasting inhibition at a hippocampal interneuron-principal neuron synapse. *Nat Neurosci* 8:1319–1328.
22. Melzer S, et al. (2012) Long-range-projecting GABAergic neurons modulate inhibition in hippocampus and entorhinal cortex. *Science* 335:1506–1510.
23. Whissell PD, Cajanding JD, Fogel N, Kim JC (2015) Comparative density of CCK- and PV-GABA cells within the cortex and hippocampus. *Front Neuroanat* 9:124.
24. Basu J, et al. (2016) Gating of hippocampal activity, plasticity, and memory by entorhinal cortex long-range inhibition. *Science* 351:aaa5694.
25. Watakabe A, et al. (2012) Area-specific substratification of deep layer neurons in the rat cortex. *J Comp Neurol* 520:3553–3573.
26. Morino P, et al. (1994) Cholecystokinin in cortico-striatal neurons in the rat: Immunohistochemical studies at the light and electron microscopical level. *Eur J Neurosci* 6:681–692.
27. Shakiryanova D, Tully A, Hewes RS, Deitcher DL, Levitan ES (2005) Activity-dependent liberation of synaptic neuropeptide vesicles. *Nat Neurosci* 8:173–178.
28. Verhage M, et al. (1991) Differential release of amino acids, neuropeptides, and catecholamines from isolated nerve terminals. *Neuron* 6:517–524.
29. Liu L, et al. (2004) Role of NMDA receptor subtypes in governing the direction of hippocampal synaptic plasticity. *Science* 304:1021–1024.
30. Lüscher C, Malenka RC (2012) NMDA receptor-dependent long-term potentiation and long-term depression (LTP/LTD). *Cold Spring Harb Perspect Biol* 4:a005710.
31. Zamanillo D, et al. (1999) Importance of AMPA receptors for hippocampal synaptic plasticity but not for spatial learning. *Science* 284:1805–1811.
32. Liu X, et al. (2012) Optogenetic stimulation of a hippocampal engram activates fear memory recall. *Nature* 484:381–385.
33. Ramirez S, et al. (2013) Creating a false memory in the hippocampus. *Science* 341:387–391.
34. Andersen P, Sundberg SH, Sveen O, Wigström H (1977) Specific long-lasting potentiation of synaptic transmission in hippocampal slices. *Nature* 266:736–737.
35. Redondo RL, Morris RG (2011) Making memories last: The synaptic tagging and capture hypothesis. *Nat Rev Neurosci* 12:17–30.
36. Horinouchi Y, et al. (2004) Reduced anxious behavior in mice lacking the CCK2 receptor gene. *Eur Neuropsychopharmacol* 14:157–161.
37. Frankland PW, Josselyn SA, Bradwejn J, Vaccarino FJ, Yeomans JS (1997) Activation of amygdala cholecystokininB receptors potentiates the acoustic startle response in the rat. *J Neurosci* 17:1838–1847.
38. Josselyn SA, et al. (1995) The CCKB antagonist, L-365,260, attenuates fear-potentiated startle. *Peptides* 16:1313–1315.
39. Chen X, et al. (2013) Encoding and retrieval of artificial visuoauditory memory traces in the auditory cortex requires the entorhinal cortex. *J Neurosci* 33:9963–9974.
40. Higuchi S, Miyashita Y (1996) Formation of mnemonic neuronal responses to visual paired associates in inferotemporal cortex is impaired by perirhinal and entorhinal lesions. *Proc Natl Acad Sci USA* 93:739–743.
41. Suthana N, et al. (2012) Memory enhancement and deep-brain stimulation of the entorhinal area. *N Engl J Med* 366:502–510.
42. Zhao C, Kao JP, Kanold PO (2009) Functional excitatory microcircuits in neonatal cortex connect thalamus and layer 4. *J Neurosci* 29:15479–15488.
43. Lee HK, Kameyama K, Huganir RL, Bear MF (1998) NMDA induces long-term synaptic depression and dephosphorylation of the GluR1 subunit of AMPA receptors in hippocampus. *Neuron* 21:1151–1162.